Temperature, doping, and polarization effects on Bi $6p$ and S $3p$ states in the BiS$_2$-layered superconductor LaO$_{1-x}$F$_x$BiS$_2$

Y. Y. Chin,[1,*] H.-J. Lin,[1,†] Z. Hu,[2] Masanori Nagao,[3,4] Yongping Du,[5] Xiangang Wan,[5] B.-J. Su,[1]
L. Y. Jang,[1] T. S. Chan,[1] H.-Y. Chen,[1] Y. L. Soo,[6] and C. T. Chen[1]

[1]*National Synchrotron Radiation Research Center, 101 Hsin-Ann Road, Hsinchu 30076, Taiwan*

[2]*Max-Planck-Institut für Chemische Physik fester Stoffe, Nöthnitzer Str. 40, Dresden 01187, Germany*

[3]*Center for Crystal Science and Technology, University of Yamanashi, 7-32 Miyamae, Kofu 400-8511, Japan*

[4]*National Institute for Materials Science, 1-2-1 Sengen, Tsukuba 305-0047, Japan*

[5]*Department of Physics and National Laboratory of Solid State Microstructures, Collaborative Innovation Center of Advanced Microstructures, Nanjing University, Nanjing 210093, People's Republic of China*

[6]*Department of Physics, National Tsing Hua University, 101 Section 2 Kuang-Fu Road, Hsinchu 30013, Taiwan*

The x-ray absorption spectra at the Bi-L_1 and S-K edges of LaO$_{1-x}$F$_x$BiS$_2$ show a decrease of spectral weight close to the absorption thresholds upon F substitution for O, indicating a reduction of the unoccupied Bi $6p$ and S $3p$ states, as expected for electron doping. This doping-induced spectral weight transfer at the S-K edge is similar to the electron-doped cuprate superconductor, Nd$_{2-x}$Ce$_x$CuO$_4$, but the polarization-dependent XAS spectra of LaO$_{0.54}$F$_{0.46}$BiS$_2$ at the S-K edge is very different from those of Nd$_{2-x}$Ce$_x$CuO$_4$ at the O-K edge, reflecting different constitution of valence electrons. We found that one-electron band structure calculations cannot describe our experimental S-K XAS spectra of LaO$_{1-x}$F$_x$BiS$_2$, suggesting possible correlation effects for p electrons, which is important in transition metal compounds with the dominating d electrons.

I. INTRODUCTION

High transition temperature (T_C) cuprates and Fe-based superconductors both have layered structures and thus exhibit exotic physical properties due to the low-dimensional electronic states [1–7]. After the discovery of superconductivity in La$_{2-x}$Ba$_x$CuO$_4$, enormous efforts were paid to enhance T_C by altering the spacer layers as well as the number of the superconducting layers and optimizing the distance between the layers [1–4]. Those studies provide us with the pathway to discover new high-T_C superconductors in two-dimensional systems at insulator-metal boundaries.

In 2012, the BiS$_2$ layer-based superconductor was found as Bi$_4$O$_4$S$_3$ which is composed of an alternate stacking of the superconducting BiS$_2$ layers and the Bi$_4$O$_4$(SO$_4$)$_{1-x}$ blocking layers, where x indicates the lack of SO$_4^{2-}$ ions at the interlayer sites [8,9]. The parent compound Bi$_6$O$_8$S$_5$ is a band insulator while displaying superconductivity through electron doping [8]. The sandwich structure resembles those of high T_C cuprates and Fe-based superconductors, where the spacer layers provide carriers to the superconducting layers, giving rise to exotic superconductivity. By changing spacer layers, another BiS$_2$-based superconductor, LaO$_{1-x}$F$_x$BiS$_2$, was synthesized afterwards [10]. Similar to Bi$_4$O$_4$S$_3$, the parent phase of LaOBiS$_2$ is a band insulator with a layered structure which consists of slabs of BiS$_2$-La$_2$O$_2$-BiS$_2$. The coupling between the two adjacent BiS$_2$ layers is weak due to van der Waals interactions [11]. Superconductivity could be achieved by a partial F substitution at the O site as electron doping [10].

In the case of the Fe-based superconductors, it was known that indirect doping into the spacer layer is more effective than direct doping in the FeAs layer, and the structural change induced by the chemical pressure is very critical for superconductivity [12,13]. In LaO$_{1-x}$F$_x$BiS$_2$, superconductivity is induced by the F substitution, which leads to the charge transfer from the LaO layer to the adjacent BiS$_2$ one and thus promotes the metallization for the BiS$_2$ layer [14]. More importantly, F substitution leads to a monotonic decrease of the c-axis lattice parameter and an anisotropic lattice deformation [15–20]. This indicates a correlation between the local structural distortion and T_C.

Different from the high T_C cuprates, where the Cu $3d$-O $2p$ states determine their transport properties, the electronic structures close to the Fermi energy in BiS$_2$ systems are dominated by the Bi $6p$-S $3p$ orbitals. The Bi $6p$-S $3p$ hybridization enhances the delocalization of the charge carriers in the BiS$_2$ plane. Both tight-binding model and density-functional calculations indicated the nesting of the Fermi surface in BiS$_2$ systems [21,22]. The μSR experiments confirmed the two-dimensional character and proposed the presence of the s-wave pairing [23]. Furthermore, the pairing strength is enhanced toward the boundary between insulator and superconductor [15].

Regarding the charge-carrier characteristics in the BiS$_2$ superconductors, the Hall resistivity experiments demonstrated that the electrons are the dominating charge carriers in NdO$_{1-x}$F$_x$BiS$_2$ and CeO$_{1-x}$F$_x$BiS$_2$ [17,18]. Moreover, the angle-resolved photoemission spectroscopy studies on LaO$_{0.54}$F$_{0.46}$BiS$_2$ and NdO$_{0.5}$F$_{0.5}$BiS$_2$ suggested that the spin-orbit coupling dictates the electronic structures and the electron correlation is rather weak [24,25].

As known from the studies on the cuprate superconductors, x-ray absorption spectroscopy (XAS) at the Cu-$L_{2,3}$ and O-K edges is a powerful tool to explore electronic structures

*chin.yiying@nsrrc.org.tw
†hjlin@nsrrc.org.tw

and provides important information about the distribution of the holes (electrons) doped in the Cu-O plane. Particularly, the polarization-dependent Cu-$L_{2,3}$ and O-K XAS spectra demonstrated the anisotropy of the unoccupied states [26–28]. In this study, we will utilize Bi-L_1 and S-K XAS to explore the distribution of the unoccupied states of the LaO$_{1-x}$F$_x$BiS$_2$ system to understand the origin of the superconducting behavior in the BiS$_2$-based materials.

II. EXPERIMENTS

LaOBiS$_2$ polycrystalline sample was synthesized using the solid-state reaction method. La$_2$S$_3$ (99.9%) powder, Bi$_2$O$_3$ (99.9%) powder, and Bi$_2$S$_3$ (99.9%) powder were mixed in a nominal composition of LaOBiS$_2$ using a mortar and sealed into a quartz tube in vacuum. Then the sample was heated at 800 °C for 10 hours. The product was ground, mixed, pressed into pellets, and heated again in an evacuated quartz tube at 900 °C for 20 hours. On the other hand, the LaO$_{0.54}$F$_{0.46}$BiS$_2$ single crystal sample was grown using CsCl/KCl flux [29]. The T_C of LaO$_{0.54}$F$_{0.46}$BiS$_2$ single crystal was measured by a superconducting quantum interface device (SQUID) magnetometer, with an applied magnetic field of 10 Oe parallel to the ab plane, and T_C was 3.0 K.

The Bi-L_1 XAS spectra were recorded at the BL07A equipped with an Si(111) double crystal monochromator providing x-ray in the photon energy range from 5 to 23 keV at the National Synchrotron Radiation Research Center (NSRRC) in Taiwan. The experimental energy resolution at
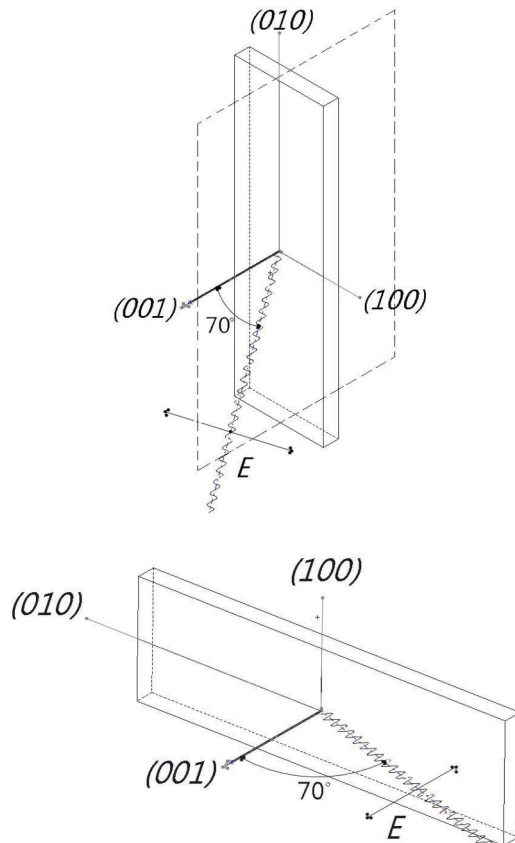

FIG. 1. Experimental geometry for $E\perp C$ (top) and $E\|C$ (bottom).

the Bi-L_1 edge (around 16 380 eV) is about 5 eV. The S-K XAS spectra were collected at the BL16A beamlines using an Si(111) double crystal monochromator, which is optimized in the photon energy range from 2 keV to 6 keV. The energy resolution at the S-K edge (around 2460 eV) is set to be 0.5 eV. The sample was mounted on a wedge, making the surface normal of the sample an angle of 70° with respect to the incoming Poynting vector. The geometry of the $E\perp C$ measurements is depicted in the top panel of Fig. 1. In this geometry, the spectrum ($I_{E\perp C}$) obtained is $E\perp C$ exclusively. For $E\|C$ experiments, we rotated the sample along the incoming beam, and the experimental geometry is shown in the bottom panel of Fig. 1. For this geometry, from the measured spectrum I$_m$ we can obtain I$_{E\|C}$ spectrum using the formula I$_{E\|C}$ = (I$_m$-I$_{E\perp C}$cos^2(70°))/sin^2(70°). This experimental setup guarantees the same beam spot on the sample for the polarization-dependence measurements, making a reliable comparison of the spectral features. The isotropic spectra can be obtained as I$_{E\|C}$ + 2I$_{E\perp C}$. All S-K XAS spectra are measured with the fluorescence yield.

III. RESULTS AND DISCUSSION

A. The doping-dependent Bi-L_1 edge XAS

The valence electrons are mainly contributed by Bi 6p states mixed with S 3p states. The former can be reached from Bi 2s core level according to the dipole selection rules in the x-ray absorption process. Therefore, the Bi-L_1 XAS is here first utilized to investigate the variation of the electronic structures via the F substitution. Figure 2(a) shows the Bi-L_1 XAS spectra of LaO$_{1-x}$F$_x$BiS$_2$ ($x = 0.0$ and 0.46). A background was removed from those spectra by subtracting a straight line fitting to the pre-edge region. The spectra were set to be zero below the absorption edges and normalized at 100 eV above the absorption edges. One can see that the Bi-L_1 XAS near-edge spectrum contains one broad peak, and its intensity decreases with the F substitution. Our observation indicates the reduction of the unoccupied 6p states upon electron doping, similar to the La^{3+} substitution for Sr^{2+} in Sr$_{1-x}$La$_x$FBiS$_2$ [15]. Therefore, the F substitution indeed dopes electrons into the BiS$_2$ superconducting layer. This is in agreement with the predictions that the doped electrons are dominating charge carriers near the Fermi surface in the electron-doped BiS$_2$-based superconductors [17,18]. Compared with the Cu-$L_{2,3}$ XAS spectra of cuprate superconductors, the Bi-L_1 XAS spectrum in Fig. 2(a) is very broad due to a poor experimental resolution and the lifetime broadening of the Bi-2s core hole as well as the broad Bi 6p states [26,27]. To extract more detailed information about the anisotropic unoccupied states and their modification upon electron doping and lowering temperature, we concentrate on the S-K XAS, which detects transitions from S-1s core level to the unoccupied S-3p states. For S^{2-} with completely filled 3p shell, the transition probability from 1s to 3p is null and becomes finite via the covalent hybridization between S 3p and Bi 6p.

B. The doping-dependent S-K edge XAS

In the high T_C cuprate superconductors, the distribution of the doped holes was well studied by O-K XAS spectra [27].
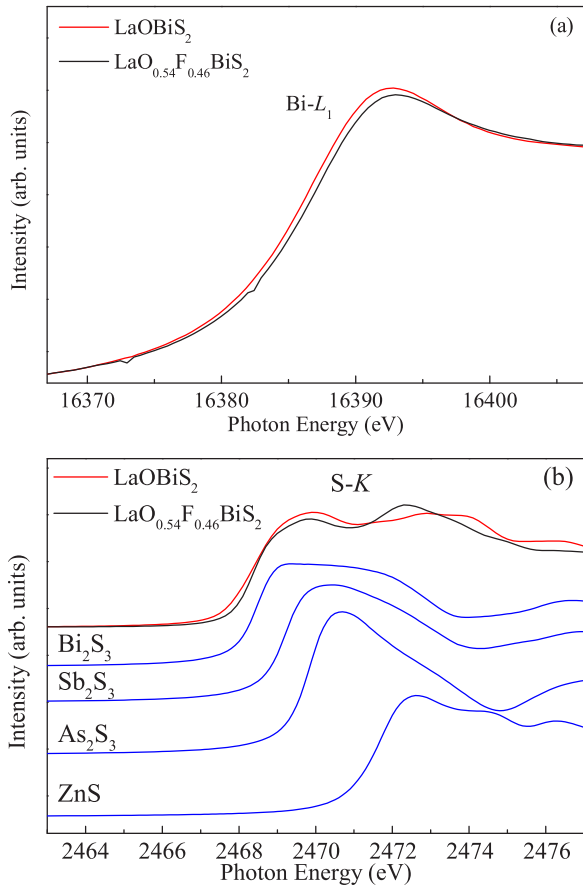
FIG. 2. (a) Experimental Bi-L_1 XAS spectra of LaO$_{1-x}$F$_x$BiS$_2$ ($x = 0.0$ and 0.46). (b) Experimental S-K XAS spectra of LaO$_{1-x}$F$_x$BiS$_2$ ($x = 0.0$ and 0.46) together with those of Bi$_2$S$_3$, Sb$_2$S$_3$, As$_2$S$_3$, and ZnS.

As a comparison, the S-K XAS spectra of the BiS$_2$-based superconductors are less documented, resulting in the indetermination concerning the location of the doped carrier. Figure 2(b) presents the S-K XAS spectra of LaO$_{1-x}$F$_x$BiS$_2$ ($x = 0.0$ and 0.46) together with those of N_2S$_3$ (N=As, Sb, and Bi) series and also that of ZnS for comparison. One can see the advantage of the S-K XAS spectra as compared with the Bi-L_1 edge in Fig. 2(a). The spectral features in the S-K edge are much better resolved. In ZnS, the Zn 3d and S 3p shells are fully occupied and therefore no 3p-related spectral intensity is expected, similar to the O-K XAS spectrum of ZnO [30,31]. Hence, the first peak in the S-K XAS spectra of the N_2S$_3$ system, located at lower photon energies compared with that of ZnS, could be assigned to the S 3p holes induced by the covalent mixing between S 3p and As 4p (Sb 5p, and Bi 6p). From As$_2$S$_3$ to Sb$_2$S$_3$, and further to Bi$_2$S$_3$, we observed a gradual energy shift of this peak to lower photon energies, indicating a gradual reduction of the band gap and also a gradual broadening of the spectral features, consistent with the resistivity data of the N_2S$_3$ [32,33]. Please note that even though all the N_2S$_3$ compounds have N^{3+}, their S-K XAS spectra locate at different photon energies. The first feature in the S-K XAS spectrum of LaOBiS$_2$ locates at the same photon energy as Bi$_2$S$_3$, reflecting the presence of the Bi^{3+}

state in LaOBiS$_2$. Furthermore, the intensity of the first peak is reduced upon the F substitution, demonstrating the decrease of the unoccupied S 3p states close to the Fermi energy, consistent with electron doping upon F substitution for O in LaO$_{1-x}$F$_x$BiS$_2$. Moreover, we have observed an increase of the spectral weight from 2471 to 2473 eV upon F substitution. In total, the spectral weight is nearly unchanged, indicating that the F substitution does not affect the in-plane Bi-S bond length remarkably, but otherwise the spectral intensity at the S-K edge would change significantly, as known in the previous study on LiTiS$_2$ [34]. It is consistent with the invariance of lattice constant a with F substitution in LaOBiS$_2$ and NdOBiS$_2$ [10,16,19]. Therefore, the invariance of a and a monotonic decrease of c through the F substitution result in the anisotropic deformation from LaOBiS$_2$. As observed in the single-crystal x-ray diffraction experiments, the increase of the F content indeed modifies the structure of the Bi-S plane, which becomes nearly flat when $x = 0.46$ [35]. The flat plane would lead to the enhancement of the hybridization of the Bi 6p$_x$/6p$_y$ and S 3p$_x$/3p$_y$ orbitals and might be responsible for the superconductivity.

Please note that there is no obvious energy shift of the S-K XAS spectrum due to the F substitution. This disproves one-electron band structure calculations, which proposed a rigid shift of the unoccupied band upon F substitution [21,22]. This disagreement might come from the electron-electron correlation. The spectroscopic behavior of the S-K XAS of LaO$_{1-x}$F$_x$BiS$_2$ is very different from that of the well-known hole-doped cuprate superconductors, where an extra peak emerges below the pre-edge of the parent compound [upper Hubbard band (UHB)], originated from Cu 3d-O 2p hybridization [26,27]. On the contrary, LaO$_{1-x}$F$_x$BiS$_2$ is similar to the electron-doped cuprate, Nd$_{2-x}$Ce$_x$CuO$_4$, where upon electron doping the spectral weight above UHB increases, filling the valley between UHB and the Nd 5d-related band [36]. Furthermore, the spectral weight transfers to the higher energies upon F substitution for O is more obvious than that upon Ce substitution for Nd in Nd$_{2-x}$Ce$_x$CuO$_4$ [36]. Although there is a difference between Cu 3d-O 2p and Bi 6p-S 3p hybridizations, the similar spectral behaviors upon electron doping suggest possible correlation effects in the p-related valence electrons. The doping dependent S-K XAS spectra in Fig. 2(b) provide a direct evidence of the significant modifications of the electronic structures via the electron doping. Considering that LaO$_{1-x}$F$_x$BiS$_2$ is composed of slabs of BiS$_2$-La$_2$(O,F)$_2$-BiS$_2$, such a layer structure would result in orbital polarization, which could be detected by the polarization-dependent XAS, as known in the O-K XAS spectra of electron-doped cuprate superconductor Nd$_{2-x}$Ce$_x$CuO$_4$ [28,36].

C. The polarization-dependent S-K edge XAS

The polarization-dependent S-K XAS spectra of LaO$_{1-x}$F$_x$BiS$_2$ are expected to provide us the detailed information of the anisotropic orbital occupations by virtue of the dipole selection rules. Figure 3(a) shows the polarization-dependent S-K edge spectra of LaO$_{0.54}$F$_{0.46}$BiS$_2$. It is quite surprising that the polarization-dependent S-K XAS from $E\|C$ to $E\perp C$ in Fig. 3(a) is very similar to the doping
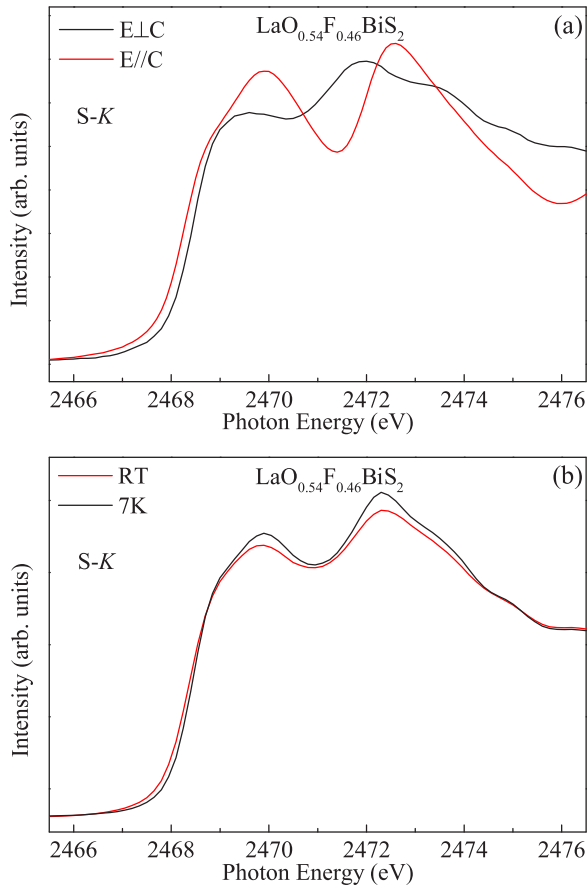
FIG. 3. (a) Polarization dependent S-K XAS spectra of LaO$_{0.54}$F$_{0.46}$BiS$_2$. (b) Experimental S-K XAS spectra of LaO$_{0.54}$F$_{0.46}$BiS$_2$ at 7 K and RT.

dependence from $x = 0$ to $x = 0.46$ in Fig. 2(b). One can see again a decrease of spectral weight below the peak at 2470 eV and an increase of spectral weight above it, namely a spectral weight transferring from lower energies to higher energies from $E\|C$ to $E\perp C$. It is worth noting that the S-K XAS probes indirectly the Bi $6p$ states through Bi $6p$-S $3p$ hybridization, and thus our experimental observation suggests that a decrease of unoccupied Bi $6p$ states occurs mainly in the *ab* plane upon electron doping. This polarization-dependent behavior is quite different from that of the electron-doped cuprate Nd$_{2-x}$Ce$_x$CuO$_4$, where one can see the significant spectral weight at the threshold when measured with $E\|ab$, while the intensity of the $E\|C$ is almost zero [28]. On the other hand, the polarization dependence of the iron pnictide, BaFe$_{1-x}$Co$_x$As, is difficult to observe [37].

Furthermore, the polarization dependence in LaO$_{0.54}$F$_{0.46}$BiS$_2$ was expected to be related to the large superconducting anisotropy observed in the BiS$_2$-based superconductors [38,39]. Although high-T_C cuprates, iron-based, and BiS$_2$-based superconductors all have layer structures, they present different physical properties. The in-plane resistivity of cuprate based superconductors and BiS$_2$-based superconductors [38,39] is much smaller than the out-of-plane one, while there is relatively weak anisotropy in the 1111-type iron-based superconductors [40–45]. The

divergence is originated from the dominating electrons around the Fermi surface. For LaO$_{1-x}$F$_x$BiS$_2$, the Fermi surface is mainly composed of the Bi $6p$ orbitals hybridized with the S $3p$ orbitals, while the electronic structures in LaO$_{1-x}$F$_x$FeAs are dominated by a complicated tangle of five Fe $3d$ orbitals [46]. The mixture of those orbitals would result in the characteristic weak anisotropy in the iron-based superconductors even with the layer structures, while the F substitution in LaO$_{1-x}$F$_x$BiS$_2$ enhances the hybridization between the Bi 6p$_x$/6p$_y$ and S 3p$_x$/3p$_y$ orbitals and results in orbital anisotropy. Although the Fermi level in high T_C cuprates is also determined by the $3d$ orbital, the holes only locate at Cu $d_{x^2-y^2}$. As a result, the layer structures in cuprates would directly induce the strong anisotropy in resistivity as well as strong polarization dependence found in the XAS experiments [26–28].

D. The temperature-dependent S-K edge XAS

To study the change of the electron structures from the normal state toward the superconducting state, we have measured the S-K XAS experiments on LaO$_{0.54}$F$_{0.46}$BiS$_2$ at different temperatures. The XAS spectra at room temperature (red) and at 7 K (black) are presented in Fig. 3(b). Compared with the strong polarization dependence at the S-K edge, the difference between the S-K spectra at RT and 7 K is relatively small. One can observe that there is a slight decrease of the spectral weight at the leading edge, as shown in Fig. 3(b). Hence, the number of electrons, the dominating charge carriers, close to the Fermi level increases toward the superconducting state. To our knowledge, there is no temperature-dependent XAS study at the O-K edge on the electron-doping high T_C cuprates for comparison. Moreover, the first feature around 2470 eV moves to higher photon energy when the sample is cooled down to 7 K. Such an energy shift is not observed in the studies on Ba$_2$Sr$_2$CaCu$_2$O$_8$ and YBa$_2$Cu$_3$O$_{6.8}$ [47,48]. The observed energy shift about 100 meV is much larger than the expected superconducting band gap. It might be related to the core-level shift or the presence of the pseudogap [49–52].

Here, we would like to draw a conclusion from our experimental XAS spectra of LaO$_{1-x}$F$_x$BiS$_2$. We have observed that F substitution leads to a decrease of the unoccupied density of states close to the Fermi energy reflecting an increase of the number of electrons close to the Fermi energy. The polarization-dependent S-K XAS spectra show that the unoccupied density of states of LaO$_{1-x}$F$_x$BiS$_2$ is lower in the *ab* plane than those of out-of-plane, indicating more electrons in the *ab* plane. This is consistent with the transport experiments, which show that the electrons are the dominating charge carriers in the superconducting state [17,18].

E. Band structure calculations

To have further understanding about the doping and polarization-dependent S-K XAS spectra of LaO$_{1-x}$F$_x$BiS$_2$, we have performed several band structure calculations with structure optimization to obtain the unoccupied density of states. First, the density of states (DOS) of S $3p$ above the Fermi energy based on the local-density approximation (LDA)
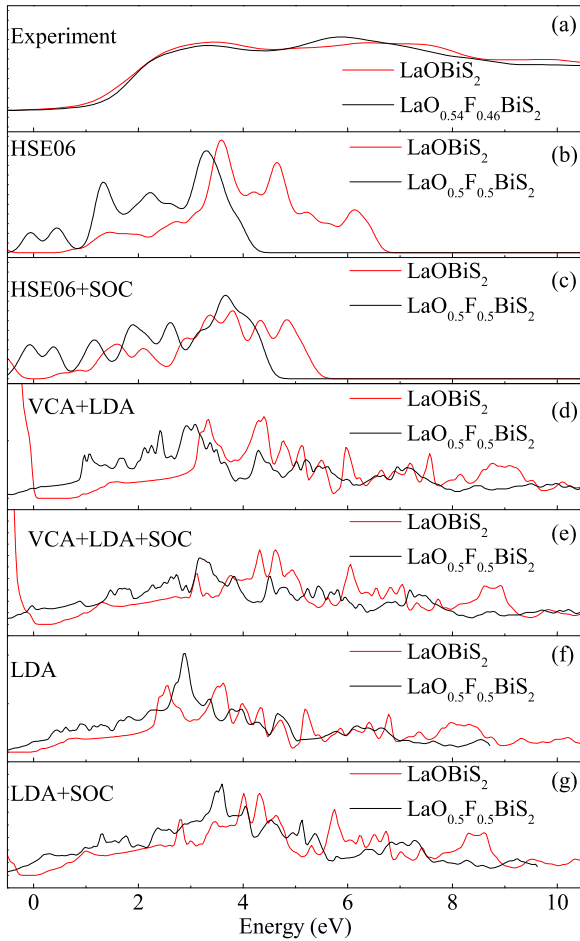
FIG. 4. (a) The S-K XAS spectra of LaOBiS$_2$ (red) and LaO$_{0.5}$F$_{0.5}$BiS$_2$ (black); (b) to (g) the theoretical results of DOS of S in LaOBiS$_2$ (red) and LaO$_{0.5}$F$_{0.5}$BiS$_2$ (black); (f) and (g) calculated by LDA scheme without and with spin-orbit coupling (SOC); (d) and (e) calculated by VCA+LDA method without and with SOC; (b) and (c) calculated by HSE06 method without and with SOC. For simplifying our calculation, we calculate the DOS neglecting the 4f state of La when applying the HSE06 method. So there is no DOS at higher energies.

without and with spin-orbit coupling (SOC) are presented in Figs. 4(f) and 4(g), respectively [53]. One could observe a lower energy shift of the unoccupied states upon electron doping from LaOBiS$_2$ (red) to LaO$_{0.5}$F$_{0.5}$BiS$_2$ (black) in Figs. 4(f) and 4(g), in agreement with previous band structure calculations. Not only the LDA, but also the virtual crystal approximation (VCA) shown in Figs. 4(d) and 4(e) predicts the shift of the Fermi level [54]. This lower energy shift results in an increase of the unoccupied state close to the Fermi energy. This is very different from our experimental S-K XAS spectra depicted in Fig. 4(a) (moved by 2466.5 eV

to be compared with the calculated density of states), which do not show such a lower energy shift of the absorption edge, but show a slight decrease of spectral weight at the leading edge upon the F substitution in contrast to the theoretical expectation. One problem of the most commonly applied functional under the LDA is that the LDA fails to cancel the self-interaction error (SIE) [55]. On the other hand, with the correction of the SIE, hybrid function scheme had been shown superior to the LDA in describing the electronic and magnetic properties [56–59]. Thus we apply the HSE06 (Heyd-Scuseria-Ernzerhof) to calculate the density of S 3p above the Fermi energy without [Fig. 4(b)] and with SOC [Fig. 4(c)], respectively [58,59]. However, the results based on HSE06 also indicate the presence of the low energy shift, similar to the conclusion in the LDA scheme as well as the VCA, shown in Figs. 4(d)–4(g). This means that one electron picture is insufficient to describe LaO$_{1-x}$F$_x$BiS$_2$. Electron correlation effects are important for 3d transition metal compounds but generally neglected for systems with dominating p valence electrons. However, the importance of Coulomb interactions for p valence electrons was indicated in the study on SrO$_{1-x}$N$_x$ [60]. Moreover, the polarization-dependent angle-resolved photoemission spectroscopy study also observed the poor agreement between the experimental data and the band structure calculations and suggested the importance of the electronic correlation and electron-phonon coupling [61].

IV. SUMMARY

To summarize, we have observed significant doping and polarization dependence in the S-K XAS spectra of LaO$_{1-x}$F$_x$BiS$_2$. The electron doping with F substitution for O results in a decrease of the spectral weight at the leading edge of the S-K XAS spectra, demonstrating a decrease of the unoccupied S 3p states close to the Fermi energy. Moreover, there is spectral weight transfer to higher photon energies, similar to the O-K XAS results of the electron doped cuprate superconductor Nd$_{2-x}$Ce$_x$CuO$_4$. The polarization-dependent S-K XAS spectra show a relatively lower spectral weight at the leading edge for $E \perp C$ compared with $E \| C$, different from the O-K XAS spectra of Nd$_{2-x}$Ce$_x$CuO$_4$, which shows a strong intensity only for $E \perp C$. The observed spectral change upon electron doping in LaO$_{1-x}$F$_x$BiS$_2$ is very different from one electron band structure calculations, suggesting the possible electron correlation effects in BiS$_2$-based superconductors.

[1] J. B. Bednorz and K. Müller, Z. Phys. B **64**, 189 (1986).

[2] M. K. Wu, J. R. Ashburn, C. J. Torng, P. H. Hor, R. L. Meng, L. Gao, Z. J. Huang, Y. Q. Wang, and C. W. Chu, Phys. Rev. Lett. **58**, 908 (1987).

[3] H. Maeda, Y. Tanaka, M. Fukutomi, and T. Asano, Jpn. J. Appl. Phys. **27**, L209 (1988).

[4] A. Schilling, M. Cantoni, J. D. Guo, and H. R. Ott, Nature (London) **363**, 56 (1993).

[5] Y. Kamihara, T. Watanabe, M. Hirano, and H. Hosono, J. Am. Chem. Soc. **130**, 3296 (2008).

[6] X. H. Chen, T. Wu, G. Wu, R. H. Liu, H. Chen, and D. F. Fang, Nature (London) **453**, 761 (2008).

[7] Z.-A. Ren, W. Lu, J. Yang, W. Yi, X.-L. Shen, C. Zheng, G.-C. Che, X.-L. Dong, L.-L. Sun, F. Zhou, and Z.-X. Zhao, Chin. Phys. Lett. **25**, 2215 (2008).

[8] Y. Mizuguchi, H. Fujihisa, Y. Gotoh, K. Suzuki, H. Usui, K. Kuroki, S. Demura, Y. Takano, H. Izawa, and O. Miura, Phys. Rev. B **86**, 220510(R) (2012).

[9] S. K. Singh, A. Kumar, B. Gahtori, G. Sharma, S. Patnaik, and V. P. S. Awana, J. Am. Chem. Soc. **134**, 16504 (2012).

[10] Y. Mizuguchi, S. Demura, K. Deguchi, Y. Takano, H. Fujihisa, Y. Gotoh, H. Izawa, and O. Miura, J. Phys. Soc. Jpn. **81**, 114725 (2012).

[11] Q. Liu, Y. Guo, and A. J. Freeman, Nano Lett. **13**, 5264 (2013).

[12] S. A. J. Kimber, A. Kreyssig, Y.-Z. Zhang, H. O. Jeschke, R. Valenti, F. Yokaichiya, E. Colombier, J. Yan, T. C. Hansen, T. Chatterji, R. J. McQueeney, P. C. Canfield, A. I. Goldman, and D. N. Argyriou, Nat. Mater. **8**, 471 (2009).

[13] C.-H. Lee, A. Iyo, H. Eisaki, H. Kito, M. T. Fernandez-Diaz, T. Ito, K. Kihou, H. Matsuhata, M. Braden, and K. Yamada, J. Phys. Soc. Jpn. **77**, 083704 (2008).

[14] I. R. Shein and A. L. Ivanovskii, JEPT Lett. **96**, 769 (2012).

[15] H. Sakai, D. Kotajima, K. Saito, H. Wadati, Y. Wakisaka, M. Mizumaki, K. Nitta, Y. Tokura, and S. Ishiwata, J. Phys. Soc. Jpn. **83**, 014709 (2014).

[16] K. Deguchi, Y. Mizuguchi, S. Demura, H. Hara, T. Watanabe, S. J. Denholme, M. Fujioka, H. Okazaki, T. Ozaki, H. Takeya, T. Yamaguchi, O. Miura, and Y. Takano, Europhys. Lett. **101**, 17004 (2013).

[17] J. Xing, S. Li, X. Ding, H. Yang, and H.-H. Wen, Phys. Rev. B **86**, 214518 (2012).

[18] R. Jha and V. P. S. Awana, Mater. Res. Express **1**, 016002 (2014).

[19] S. Demura, Y. Mizuguchi, K. Deguchi, H. Okazaki, H. Hara, T. Watanabe, S. J. Denholme, M. Fujioka, T. Ozaki, H. Fujihisa, Y. Gotoh, O. Miura, T. Yamaguchi, H. Takeya, and Y. Takano, J. Phys. Soc. Jpn. **82**, 033708 (2013).

[20] J. Kajitani, T. Hiroi, A. Omachi, O. Miura, and Y. Mizuguchi, J. Phys. Soc. Jpn. **84**, 044712 (2015).

[21] H. Usui, K. Suzuki, and K. Kuroki, Phys. Rev. B **86**, 220501(R) (2012).

[22] X. Wan, H.-C. Ding, S. Y. Savrasov, and C.-G. Duan, Phys. Rev. B **87**, 115124 (2013).

[23] G. Lamura, T. Shiroka, P. Bonfà, S. Sanna, R. De Renzi, C. Baines, H. Luetkens, J. Kajitani, Y. Mizuguchi, O. Miura, K. Deguchi, S. Demura, Y. Takano, and M. Putti, Phys. Rev. B **88**, 180509(R) (2013).

[24] K. Terashima, J. Sonoyama, T. Wakita, M. Sunagawa, K. Ono, H. Kumigashira, T. Muro, M. Nagao, S. Watauchi, I. Tanaka, H. Okazaki, Y. Takano, O. Miura, Y. Mizuguchi, H. Usui, K. Suzuki, K. Kuroki, Y. Muraoka, and T. Yokoya, Phys. Rev. B **90**, 220512(R) (2014).

[25] Z. R. Ye, H. F. Yang, D. W. Shen, J. Jiang, X. H. Niu, D. L. Feng, Y. P. Du, X. G. Wan, J. Z. Liu, X. Y. Zhu, H. H. Wen, and M. H. Jiang, Phys. Rev. B **90**, 045116 (2014).

[26] C. T. Chen, F. Sette, Y. Ma, M. S. Hybertsen, E. B. Stechel, W. M. C. Foulkes, M. Schluter, S. W. Cheong, A. S. Cooper, L. W. Rupp, B. Batlogg, Y. L. Soo, Z. H. Ming, A. Krol, and Y. H. Kao, Phys. Rev. Lett. **66**, 104 (1991).

[27] C. T. Chen, L. H. Tjeng, J. Kwo, H. L. Kao, P. Rudolf, F. Sette, and R. M. Fleming, Phys. Rev. Lett. **68**, 2543 (1992).

[28] E. Pellegrin, N. Nucker, J. Fink, S. L. Molodtsov, A. Gutierrez, E. Navas, O. Strebel, Z. Hu, M. Domke, G. Kaindl, S. Uchida, Y. Nakamura, J. Markl, M. Klauda, G. Saemann-Ischenko, A. Krol, J. L. Peng, Z. Y. Li, and R. L. Greene, Phys. Rev. B **47**, 3354 (1993).

[29] M. Nagao, A. Miura, S. Demura, K. Deguchi, S. Watauchi, T. Takei, Y. Takano, N. Kumada, and I. Tanaka, Solid State Commun. **178**, 33 (2014).

[30] C. L. Dong, C. Persson, L. Vayssieres, A. Augustsson, T. Schmitt, M. Mattesini, R. Ahuja, C. L. Chang, and J.-H. Guo, Phys. Rev. B **70**, 195325 (2004).

[31] G. S. Chang, E. Z. Kurmaev, D. W. Boukhvalov, L. D. Finkelstein, S. Colis, T. M. Pedersen, A. Moewes, and A. Dinia, Phys. Rev. B **75**, 195215 (2007).

[32] N. K. Abrikosov, V. F. Bankina, L. V. Poretskaya, L. E. Shelimova, and E. V. Skudnova, *Semiconducting IIVVI, IVVVI, and VVVI Compounds* (Springer, USA, 1969), p. 186 and p. 190.

[33] A. V. Kolobov and J. Tominaga, *Chalcogenides: Metastability and Phase Change Phenomena* (Springer, Berlin, Heidelberg, 2012), p. 36.

[34] Z. Y. Wu, G. Ouvrard, S. Lemaux, P. Moreau, P. Gressier, F. Lemoigno, and J. Rouxel, Phys. Rev. Lett. **77**, 2101 (1996).

[35] A. Miura, M. Nagao, T. Takei, S. Watauchi, I. Tanaka, and N. Kumada, J. Solid State Chem. **212**, 213 (2014).

[36] J. Fink, N. Nücker, M. Alexander, H. Romberg, M. Knupfer, M. Merkel, P. Adelmann, R. Claessen, G. Mante, T. Buslaps, S. Harm, R. Manzke, and M. Skibowski, Physica C: Superconductivity **185-189**, 45 (1991).

[37] Y. K. Kim, W. S. Jung, G. R. Han, K.-Y. Choi, C.-C. Chen, T. P. Devereaux, A. Chainani, J. Miyawaki, Y. Takata, Y. Tanaka, M. Oura, S. Shin, A. P. Singh, H. G. Lee, J.-Y. Kim, and C. Kim, Phys. Rev. Lett. **111**, 217001 (2013).

[38] M. Nagao, S. Demura, K. Deguchi, A. Miura, S. Watauchi, T. Takei, Y. Takano, N. Kumada, and I. Tanaka, J. Phys. Soc. Jpn. **82**, 113701 (2013).

[39] M. Nagao, A. Miura, S. Watauchi, Y. Takano, and I. Tanaka, Jpn. J. Appl. Phys. **54**, 083101 (2015).

[40] S. W. Tozer, A. W. Kleinsasser, T. Penney, D. Kaiser, and F. Holtzberg, Phys. Rev. Lett. **59**, 1768 (1987).

[41] Y. Iye, T. Tamegai, T. Sakakibara, T. Goto, N. Miura, H. Takeya, and H. Takei, Physica C **153**, 26 (1988).

[42] S. J. Hagen, T. W. Jing, Z. Z. Wang, J. Horvath, and N. P. Ong, Phys. Rev. B **37**, 7928(R) (1988).

[43] D. E. Farrell, S. Bonham, J. Foster, Y. C. Chang, P. Z. Jiang, K. G. Vandervoort, D. J. Lam, and V. G. Kogan, Phys. Rev. Lett. **63**, 782 (1989).

[44] B. D. Biggs, M. N. Kunchur, J. J. Lin, S. J. Poon, T. R. Askew, R. B. Flippen, M. A. Subramanian, J. Gopalakrishnan, and A. W. Sleight, Phys. Rev. B **39**, 7309(R) (1989).

[45] P. J. W. Moll, R. Puzniak, F. Balakirev, K. Rogacki, J. Karpinski, N. D. Zhigadlo, and B. Batlogg, Nat. Mater. **9**, 628 (2010).

[46] W. Malaeb, T. Yoshida, T. Kataoka, A. Fujimori, M. Kubota, K. Ono, H. Usui, K. Kuroki, R. Arita, H. Aoki, Y. Kamihara, M. Hirano, and H. Hosono, J. Phys. Soc. Jpn. **77**, 093714 (2008).

[47] Y. Hirai, I. Waki, A. Momose, T. Fukazawa, T. Aida, K. Takagi, and T. Hirano, Phys. Rev. B **45**, 2573(R) (1992).

[48] N. L. Saini, D. S-L. Law, P. Pudney, K. B. Garg, A. A. Menovsky, and J. J. M. Franse, Phys. Rev. B **52**, 6219 (1995).

[49] H. Ding, T. Yokoya, J. C. Campuzano, T. Takahashi, M. Randeria, M. R. Norman, T. Mochiku, K. Kadowaki, and J. Giapintzakis, Nature (London) **382**, 51 (1996).

[50] M. R. Norman, H. Ding, M. Randeria, J. C. Campuzano, T. Yokoya, T. Takeuchi, T. Takahashi, T. Mochiku, K. Kadowaki, P. Guptasarma, and D. G. Hinks, Nature (London) **392**, 157 (1998).

[51] J. Liu, M. Kargarian, M. Kareev, B. Gray, P. J. Ryan, A. Cruz, N. Tahir, Y.-D. Chuang, J. Guo, J. M. Rondinelli, J. W. Freeland, G. A. Fiete, and J. Chakhalian, Nat. Commun. **4**, 2714 (2013).

[52] E. Goering, S. Gold, M. Lafkioti, G. Schutz, and V. A. M. Brabers, Phys. Rev. B **72**, 033112 (2005).

[53] A. D. Becke, Phys. Rev. A **38**, 3098 (1988).

[54] L. Bellaiche and D. Vanderbilt, Phys. Rev. B **61**, 7877 (2000).

[55] S. Kummel and L. Kronik, Rev. Mod. Phys. **80**, 3 (2008).

[56] V. L. Chevrier, S. P. Ong, R. Armiento, M. K. Y. Chan, and G. Ceder, Phys. Rev. B **82**, 075122 (2010).

[57] M. Schlipf, M. Betzinger, M. Ležaić, C. Friedrich, and S. Blügel, Phys. Rev. B **88**, 094433 (2013).

[58] J. Heyd, G. E. Scuseria, and M. Ernzerhof, J. Chem. Phys. **118**, 8207 (2003).

[59] J. Heyd and G. E. Scuseria, J. Chem. Phys. **120**, 7274 (2004).

[60] I. S. Elfimov, A. Rusydi, S. I. Csiszar, Z. Hu, H. H. Hsieh, H.-J. Lin, C. T. Chen, R. Liang, and G. A. Sawatzky, Phys. Rev. Lett. **98**, 137202 (2007).

[61] T. Sugimoto, D. Ootsuki, C. Morice, E. Artacho, S. S. Saxena, E. F. Schwier, M. Zheng, Y. Kojima, H. Iwasawa, K. Shimada, M. Arita, H. Namatame, M. Taniguchi, M. Takahashi, N. L. Saini, T. Asano, R. Higashinaka, T. D. Matsuda, Y. Aoki, and T. Mizokawa, Phys. Rev. B **92**, 041113(R) (2015).